



Cite this: *Environ. Sci.: Water Res. Technol.*, 2020, 6, 2553

## UVC-based advanced oxidation processes for simultaneous removal of microcontaminants and pathogens from simulated municipal wastewater at pilot plant scale†

Isaac Sánchez-Montes,<sup>a</sup> Irene Salmerón García,<sup>b</sup> Gracia Rivas Ibañez,<sup>b</sup> José Mario Aquino,<sup>a</sup> María Inmaculada Polo-López,<sup>b</sup> Sixto Malato<sup>\*b</sup> and Isabel Oller<sup>\*b</sup>

The challenge of providing good-quality reclaimed water free from contaminants of emerging concern, even at small concentrations, *i.e.*, microcontaminants (MCs), and pathogens is one of the main hot topics worldwide. UVC-based advanced oxidation processes, using *in situ* production of strong oxidizing radicals, such as HO<sup>•</sup> and SO<sub>4</sub><sup>•-</sup>, have shown high oxidation rates for MCs; however, few studies have focused on the simultaneous removal of MCs and pathogens, like bacteria. Thus, the aim of this work was to assess the oxidation of six MCs, acetaminophen (ACT), caffeine, (CAF), carbamazepine (CBZ), trimethoprim (TMP), sulfamethoxazole (SMX), and diclofenac (DCF), in the presence of *Escherichia coli*, *Enterococcus faecalis*, and *Salmonella enteritidis* in a simulated effluent from a municipal wastewater treatment plant by the application of UVC/H<sub>2</sub>O<sub>2</sub> and UVC/S<sub>2</sub>O<sub>8</sub><sup>2-</sup> processes at pilot plant scale. The concentration of MCs and bacteria was monitored along the oxidation processes as well as their regrowth after 24, 48, and 144 h. UVC-based processes were compared in terms of the required treatment time to remove at least 80% of the sum of MCs, regrowth assessment, and energy consumption. Despite the UVC/H<sub>2</sub>O<sub>2</sub> and UVC/S<sub>2</sub>O<sub>8</sub><sup>2-</sup> processes showing similar results, even after using distinct molar concentrations, the UVC/H<sub>2</sub>O<sub>2</sub> process did not exhibit bacterial regrowth under dark conditions. A simple model has also been proposed in this work with the main objective of calculating the minimum concentration of oxidants as a function of the radiation absorption at 254 nm in a given photo-reactor setup.

Received 27th March 2020,  
Accepted 2nd June 2020

DOI: 10.1039/d0ew00279h

rsc.li/es-water

### Water impact

Fresh water free from microcontaminants (MCs) and pathogens is one of the main hot topics worldwide. UVC advanced oxidation processes producing strong oxidizing radicals have shown high oxidation rates; however, few studies focused on the simultaneous removal of pathogens at pilot scale. These processes were compared in terms of the required treatment time to remove at least 80% of the sum of microcontaminants, regrowth assessment, and energy consumption.

## 1. Introduction

Assurance of safe reclaimed water free of chemical and microbiological contaminants is a serious global concern that is increasing with population growth and uncertain climate changes. Wastewater effluents treated by conventional methods can contain a huge amount of microcontaminants

(MCs) (pesticides, pharmaceuticals, personal care products, *etc.*) and pathogens (bacteria, viruses, protozoa, and parasites) that may lead to toxic effects in humans when reaching fresh water sources.<sup>1–4</sup> In addition, water supplies from nontraditional sources, including treated municipal wastewater, have been proposed as feasible options in recent years.<sup>5,6</sup> Unfortunately, consolidated tertiary treatments such as UVC radiation, ozonation and chlorination are not effective enough or present serious drawbacks in their application to remove MCs. UVC irradiation (200–280 nm) has been extensively used for water disinfection; however, serious limitations such as microbial regrowth (due mainly to the lack of residual effect) and mechanisms of self-repair of microorganisms' DNA were observed.<sup>7,8</sup> In addition,

<sup>a</sup> Departamento de Química, Universidade Federal de São Carlos, 13565-905, São Carlos (São Paulo), Brazil

<sup>b</sup> Plataforma Solar de Almería-CIEMAT, Ctra Senés km 4.5, 04200 Tabernas, Almería, Spain. E-mail: sixto.malato@psa.es, isabel.oller@psa.es

† Electronic supplementary information (ESI) available. See DOI: 10.1039/d0ew00279h



depending on the chemical structure of the target molecule, UVC irradiation is not appropriate for MC elimination.<sup>9</sup> Chlorination and ozonation can inactivate pathogens and remove MCs, though generation of toxic disinfection by-products, e.g., organochlorine, nitrosodimethylamine, and bromate, has been their main drawback.<sup>7,10–12</sup> Other potential disinfection methods such as ultrasonication, hydrodynamic cavitation, membrane filtration, and electrochemical oxidation have been effectively used to inactivate or remove microorganisms from water as a low use of chemicals is needed;<sup>13–16</sup> however, both physical and electrochemical technologies have common shortcomings including high energy consumption and operating costs as well as the requirement of designing sophisticated reactors.

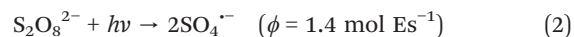
To overcome these problems, UVC-based advanced oxidation processes (UVC AOPs) represent a feasible alternative to conventional tertiary treatments.<sup>17,18</sup> UVC AOPs have been investigated for the production of a huge variety of highly reactive free radicals, e.g., HO·, Cl·, SO<sub>4</sub><sup>·-</sup>, CO<sub>3</sub><sup>·-</sup>, that lead to high elimination rates of microorganisms and contaminants.<sup>19–22</sup> In addition, commercial UVC reactors have already been used in water and wastewater treatment plants so they could be easily adapted for these processes.<sup>23</sup> In comparison with other AOPs such as Fenton and photo-Fenton, these processes do not require pH adjustments and addition of Fe ions, which simplifies operational requirements.

The UVC/hydrogen peroxide (UVC/H<sub>2</sub>O<sub>2</sub>) process is one of the most disseminated AOPs used for organic compound degradation and disinfection.<sup>24,25</sup> In this process, the non-selective HO· species can be produced from the homolytic cleavage of H<sub>2</sub>O<sub>2</sub> by absorption of UVC radiation (mainly at 254 nm), with a quantum efficiency of 0.5 mol Es<sup>-1</sup> (eqn (1)).<sup>26,27</sup> Due to its high oxidizing power ( $E^{\circ}(\text{HO}^{\cdot}/\text{H}_2\text{O}) = 1.8\text{--}2.7$  V), HO· can cause irreversible damage in microorganisms having the advantage of reacting non-selectively with organic compounds through electron transfer, hydrogen atom abstraction or electrophilic addition.<sup>28</sup>



AOPs based on sulfate radicals (SO<sub>4</sub><sup>·-</sup>) have been widely reported in the literature for removal of organic compounds, but to the best of our knowledge, there is a scarcity of studies addressing simultaneous disinfection and MC degradation.<sup>29,30</sup> This process was proposed a long time ago due to its synergistic effect with TiO<sub>2</sub> photocatalysis for conduction band electron scavenging and production of inorganic oxidizing species.<sup>31</sup> This radical has an oxidation potential ( $E^{\circ}(\text{SO}_4^{\cdot-}/\text{SO}_4^{2-}) = 2.5\text{--}3.1$  V) comparable to that of the HO· species and can be generated by the activation of persulfate (S<sub>2</sub>O<sub>8</sub><sup>2-</sup>) or peroxymonosulfate (HSO<sub>5</sub><sup>-</sup>) through heat, UVC irradiation, and transition metal species.<sup>26,32</sup> In addition, depending on the properties of the molecule, SO<sub>4</sub><sup>·-</sup> can lead to high oxidation rates of specific contaminants (particularly aromatic compounds).<sup>33</sup> The photolysis (see eqn (2)) of S<sub>2</sub>O<sub>8</sub><sup>2-</sup> by UVC light (at 254 nm) to produce SO<sub>4</sub><sup>·-</sup> occurs with a quantum yield

2.8 times higher than when using H<sub>2</sub>O<sub>2</sub>.<sup>26</sup> Generated SO<sub>4</sub><sup>·-</sup> species can readily react with H<sub>2</sub>O molecules, resulting in the production of HO· (see eqn (3)). These electrophilic species react with aromatic compounds through three main mechanisms, i.e., radical adduct formation, hydrogen atom abstraction, and single electron transfer.<sup>33</sup>



Previous studies have investigated the efficiency of different UVC AOPs (even UVC/H<sub>2</sub>O<sub>2</sub> and UVC/S<sub>2</sub>O<sub>8</sub><sup>2-</sup>) to eliminate pathogens or MCs from water. However, most of these studies applied such processes under no realistic experimental conditions, such as in pure or distilled water, at laboratory scale, and under acidic or basic pH conditions.<sup>34,35</sup> In complex matrices such as municipal wastewater, the efficiency of these technologies can be significantly reduced, mainly due to the quenching reactions between the produced free radicals and the organic matter and inorganic ions (HCO<sub>3</sub><sup>-</sup>, SO<sub>4</sub><sup>2-</sup>, Cl<sup>-</sup>, and PO<sub>4</sub><sup>3-</sup>) present in these effluents.<sup>36,37</sup> Moreover, disinfection and degradation processes have been studied independently and only very few papers reported on the concomitant achievement of MC removal and elimination of pathogens. Thus, investigation of UVC AOPs for tertiary treatment of municipal wastewater is worthy and focuses not only on microorganism inactivation results but also on the possibility of attaining simultaneous oxidation of MCs for water reusing purposes.

In this context, this work aimed to investigate and compare the use of the UVC/H<sub>2</sub>O<sub>2</sub> and UVC/S<sub>2</sub>O<sub>8</sub><sup>2-</sup> processes for the simultaneous removal of MCs and pathogens from a simulated municipal wastewater secondary effluent at pilot plant scale. *Escherichia coli*, *Enterococcus faecalis*, and *Salmonella enteritidis* were selected as target microorganisms because they are used as pathogen indicators in regulations and guidelines for wastewater disposal and reuse.<sup>38,39</sup> Six MCs, acetaminophen (ACT), caffeine (CAF), carbamazepine (CBZ), trimethoprim (TMP), sulfamethoxazole (SMX) and diclofenac (DCF), were chosen as target molecules since they are usually detected in municipal wastewater.<sup>40</sup> In addition, this work intends to compare UVC/H<sub>2</sub>O<sub>2</sub> and UVC/S<sub>2</sub>O<sub>8</sub><sup>2-</sup> processes in terms of treatment time, consumption of chemicals, and the influence of the oxidant residual concentration on the bacterial regrowth. Finally, a simple model based on the optical path length of the UVC radiation is proposed to determine the most suitable oxidant concentration to be used in these systems to simultaneously remove MCs and pathogens.

## 2. Experimental section

### 2.1 Chemicals

ACT, CBZ, TMP, SMX, and DCF were purchased from Sigma-Aldrich (>99%). Caffeine (CAF) was provided by Fluka (>99%). H<sub>2</sub>O<sub>2</sub> (35%), Na<sub>2</sub>S<sub>2</sub>O<sub>8</sub> (>98%), KI (>99.5%), Na<sub>2</sub>S<sub>2</sub>O<sub>3</sub> (>99%),



bovine liver catalase, phosphate-buffered saline, acetonitrile (UHPLC-grade), and formic acid (UHPLC-grade) were purchased from Sigma-Aldrich. All chemicals were used as received. The MC stock solution for experiments was prepared in methanol at 2.5 g L<sup>-1</sup> each to avoid hydrolysis of MCs and allow spiking low volumes of water with very low quantities of methanol in the pilot plant. Simulated municipal wastewater (SMWW) secondary effluent was used as the wastewater model. The resulting physicochemical properties of the prepared SMWW effluent are shown in Table 1.

This matrix was prepared after adaption of the procedure described in Zhang *et al.*<sup>41</sup> and in the APHA Standard Methods,<sup>42</sup> using the following chemicals:

(i) Inorganics salts: NaHCO<sub>3</sub> (96 mg L<sup>-1</sup>), MgSO<sub>4</sub> (60 mg L<sup>-1</sup>), NaCl (580 mg L<sup>-1</sup>), and K<sub>2</sub>HPO<sub>4</sub> (7.0 mg L<sup>-1</sup>) (Sigma-Aldrich); CaSO<sub>4</sub>·2H<sub>2</sub>O (60 mg L<sup>-1</sup>) and (NH<sub>4</sub>)<sub>2</sub>SO<sub>4</sub> (23.6 mg L<sup>-1</sup>) (Panreac); KCl (4 mg L<sup>-1</sup>) (J.T. Baker).

(ii) Organic matter: beef extract (1.8 mg L<sup>-1</sup>) and peptone (2.7 mg L<sup>-1</sup>) (Biolife); humic acid (4.2 mg L<sup>-1</sup>), sodium lignin sulfonate (2.4 mg L<sup>-1</sup>) and sodium lauryl sulphate (0.9 mg L<sup>-1</sup>) (Sigma-Aldrich); tannic acid (4.2 mg L<sup>-1</sup>) and acacia gum powder (4.7 mg L<sup>-1</sup>) (Panreac).

It is important to remark that SMWW characteristics are highly similar to those of the actual MWWTP effluent and selected MCs and pathogens to be monitored were spiked at concentrations in the range of those actually found in such effluents.

## 2.2 Analyses

**2.2.1 Analytical quantification of MCs.** The concentration of MCs was monitored by ultra-performance liquid chromatography with a UV-DAD detector (Agilent Technologies, Infinity Series 1200) using a Poroshell 120 EC-C18 column as the stationary phase (Agilent Technologies: 50 mm × 3.0 mm, 2.7 μm particle) and a mixture of 25 mmol L<sup>-1</sup> formic acid and acetonitrile (ACN) as the mobile phase at 1 mL min<sup>-1</sup>. A gradient elution mode was used. The initial condition was 100% formic acid 25 mmol L<sup>-1</sup>, varying in 10 min up to 50% formic acid/ACN; then in 2 min 100% ACN was reached and maintained for another 2 min. Analysis time was set to 14 min, followed by 3 min of post-time for setting the column to initial conditions. The injection volume and temperature of the column were 50 μL and 30 °C, respectively. Before sample analysis, 9 mL of collected sample were filtered using a 0.22 μm PTFE filter (Millipore) and the filter was washed with 1 mL of ACN to remove any adsorbed

compounds. The detection limit for all the compounds studied was 5 μg L<sup>-1</sup>. Other information such as retention time, maximum quantification wavelength and chromatographic area of 100 μg L<sup>-1</sup> for each MC are available in Table S1 (ESI†).

Other parameters were also monitored, such as pH (GLP 22 pH meter, CRISON), conductivity (GLP 31 conductometer, CRISON), and turbidity (2100 N turbidimeter, HACH). Dissolved organic carbon (DOC) and dissolved inorganic carbon (DIC) were measured using a TOC-VCSN analyzer (Shimadzu) in filtered samples through 0.45 μm nylon filter (AISIMO).

Ion chromatography was used to measure the concentration of various ions in samples previously filtered (0.45 μm nylon filter), using a Metrohm 850 Professional analyzer. For anion determination, a Metrosep A Supp 7150/4.0 column at 45 °C and 3.6 mmol L<sup>-1</sup> sodium carbonate at 0.7 mL min<sup>-1</sup> were used as the stationary and mobile phase, respectively. A Metrosep C6 150/4.0 column and 1.7 mmol L<sup>-1</sup> solutions of nitric acid and dipicolinic acid at 1.2 mL min<sup>-1</sup> were used for cation quantification.

The concentration of oxidants was determined by two different methods using a UV-vis Evolution 220 spectrophotometer (Thermo Scientific). H<sub>2</sub>O<sub>2</sub> concentration was analyzed spectrophotometrically at 410 nm after adding 0.5 mL of titanium(IV) oxysulfate to 5 mL of a filtered sample (DIN 38402H15). S<sub>2</sub>O<sub>8</sub><sup>2-</sup> concentration was monitored by using an iodometric method adapted from Liang *et al.*<sup>43</sup> Briefly, 3.5 mL of 50 g L<sup>-1</sup> KI solution and 0.5 mL of 5 g L<sup>-1</sup> NaHCO<sub>3</sub> solution were added to 1 mL of previously filtered sample, allowed to react for 15 min, and then the absorbance at 352 nm was measured.

**2.2.2 Bacterial quantification analysis.** Selected strains of bacteria were provided by Spanish Culture Collection (CECT): *E. coli* (O157:H7) (CECT 4972), *E. faecalis* (CECT 5143), and *S. enteritidis* (CECT 4155). These strains were used to prepare the microbial suspensions spiked in the SMWW secondary effluent. *E. coli*, *E. faecalis*, and *S. enteritidis* were inoculated in 14 mL of nutrient broth (a mixture of NaCl, beef extract, and peptone), Luria-Bertani broth (Sigma-Aldrich), and tryptone soya broth (OXOID), respectively, and grown aerobically in a rotary shaker (90 rpm) at 37 °C for 20 h. The microbial suspensions were then centrifuged at 3000 rpm (704 g) for 15 min (J.P. Selecta). The microbial pellet was re-suspended in sterilized phosphate-buffered saline (PBS) solution to give a stock suspension containing approximately 10<sup>11</sup> CFU per 100 mL. An aliquot of 100 μL of each bacterial suspension was added to the SMWW secondary effluent to obtain an initial concentration of 10<sup>5</sup> CFU per 100 mL.

Bacterial quantification was performed by the standard plate counting method using specific culture media: Chromocult® (Merck), Slanetz–Bartley agar (1% TTC) (Scharlau), and Salmonella Shigella agar (Scharlau) for *E. coli*, *E. faecalis*, and *S. enteritidis*, respectively. When the bacterial concentration expected was lower than 2 × 10<sup>2</sup> CFU per 100 mL, samples were processed by the membrane filtration method. For each bacterium, 100 mL of sample were filtered

**Table 1** Physicochemical characterization of SMWW effluent

Parameters	
pH	7.6 ± 0.3
Conductivity (mS cm <sup>-1</sup> )	1.4 ± 0.1
Turbidity (NTU)	3.4 ± 0.2
DOC (mg L <sup>-1</sup> )	15.5 ± 0.6
DIC (mg L <sup>-1</sup> )	13.5 ± 1.2



using a 0.45  $\mu\text{m}$ -pore-size cellulose nitrate membrane (Sartorius) and a Microfil filtration system (Millipore). Then, the obtained membranes were plated in the corresponding medium and incubated at 37 °C. *E. coli* colonies were counted after 24 h; *E. faecalis* and *S. enteritidis* samples were counted after 48 h. The detection limit (DL) of this technique is 1 CFU per 100 mL, taking into account the minimum disinfection level required by the Spanish legislation for reusing reclaimed wastewater (RD 1620/2007).<sup>44</sup> A control sample (without treatment) for each bacterium was plated before and after the experiment to guarantee the strain's good quality.

When oxidant reagents were used, a proportional volume of bovine liver catalase solution (0.1 g L<sup>-1</sup>) or sodium thiosulfate (10 mmol L<sup>-1</sup>) was added to the samples in order to quench residual H<sub>2</sub>O<sub>2</sub> and S<sub>2</sub>O<sub>8</sub><sup>2-</sup>, respectively. Regrowth of bacteria was quantified in predetermined samples stored at room temperature for 24, 48, and 144 h (6 days) (quencher was not added for this analysis). Disinfection experiments were carried out in duplicate and average values were plotted. The inactivation kinetics of each bacterium observed during the UVC-based treatments were calculated by using Chick–Watson's equation.<sup>45</sup> The results were reproducible and the standard deviation of the replicates is shown in the graphs as error bars.

### 2.3 UVC pilot plant description and experimental procedure

UVC, UVC/H<sub>2</sub>O<sub>2</sub>, and UVC/S<sub>2</sub>O<sub>8</sub><sup>2-</sup> experiments were carried out by using a UVC pilot plant previously described by Cerreta *et al.*<sup>46</sup> Fig. 1 shows a schematic configuration of the reactor containing the UVC lamp. The pilot plant consists of three medium pressure UVC lamps (230 W with radiation emission at 254 nm) protected by quartz tubes ( $\varnothing_{\text{int}} = 3.7$  cm) and axially located in a stainless steel cylindrical photoreactor ( $\varnothing_{\text{int}} = 8.9$  cm). The flexible design of the system allows the use of one, two or three lamps in batch or continuous flow mode. In this study, a single lamp was used in batch mode (recirculation flow rate 36 L min<sup>-1</sup>) with a total volume of 80 L.

The total irradiated surface of the photoreactor (one lamp;  $S_p = 0.34$  m<sup>2</sup>) and the illuminated volume (one lamp;  $V_{\text{illu}} = 6.21$  L) were calculated according to eqn (4) and (5) taking into account the specific characteristics of the lamp and its frame.

$$V_{\text{illu}}(\text{L}) = L_L \pi (r_{\text{int,C}}^2 - r_{\text{int,L}}^2) \quad (4)$$

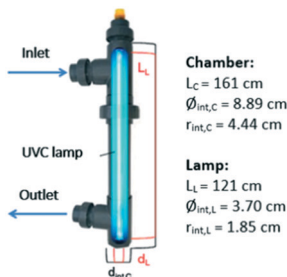


Fig. 1 UVC photoreactor scheme and main characteristics.

$$S_p(\text{m}^2) = 2\pi R_{\text{int,C}} L_L \quad (5)$$

To compare the energy consumption of these processes with other photochemical based systems, the accumulative UVC energy per L ( $Q_{\text{UVC}}$ ) was calculated according to eqn (6). For that, the incident energy rate on a surface per unit area (irradiance;  $\text{W m}^{-2}$ ) emitted by the UVC lamp was continuously monitored using a detector (ProMinent) placed in the inner wall of the cylindrical photochemical reactor. Details of the irradiance profile of the UVC lamp (maximum 85.6  $\text{W m}^{-2}$ ) measured in distilled water are shown in Fig. S1 (ESI†).

$$Q_{\text{UVC}}(\text{kJ L}^{-1}) = \text{Dose}(\text{kJ m}^{-2}) \frac{S_p(\text{m}^2)}{V_T(\text{L})} \quad (6)$$

where Dose is the product of emitted irradiance by the UVC lamp ( $\text{W m}^{-2}$ ) multiplied by the illumination time fraction (s).  $S_p$  is the total irradiated surface of the photoreactor (m<sup>2</sup>) and  $V_T$  is the total water volume (L).

In UVC AOP experiments, the system's reservoir was filled with 80 L of SMWW secondary effluent and the required quantity of a stock solution of MCs was added to obtain an initial concentration of 100  $\mu\text{g L}^{-1}$  of each compound. The sum of these concentrations for the six selected MCs is considered higher but very close to the range normally found in effluents of municipal wastewater treatment plants.<sup>47–50</sup> Then, each bacterial stock was added to obtain 10<sup>5</sup> CFU per 100 mL per bacterium. After 15 min of homogenization (UVC lamp switched off), an initial sample was taken to check the initial concentration of both MCs and bacteria. Then, H<sub>2</sub>O<sub>2</sub> (5, 15, 25, 35, and 50 mg L<sup>-1</sup>) or S<sub>2</sub>O<sub>8</sub><sup>2-</sup> (20, 40, and 100 mg L<sup>-1</sup>) was added to the reservoir tank. After homogenization (10 min), another sample was collected to verify the effect of the oxidants on the concentration of MCs and bacteria in the dark (any significant variation in initial concentrations was observed in either of the experiments performed, data not shown). Then the UVC lamp was switched on and the experiment started. Samples were collected at predetermined and regular time intervals to analyze simultaneously the degradation of MCs, inactivation of bacteria and reagent evolution along all the UVC-based experiments performed in this study.

## 3. Results and discussion

### 3.1 UVC treatment

Results of simultaneous inactivation of bacteria and degradation of MCs using only UVC light in the SMWW secondary effluent are depicted in Fig. 2. A high inactivation rate of *E. coli*, *E. faecalis*, and *S. enteritidis* was obtained under UVC irradiation. The strong effect of the UVC light (mainly at 254 nm) observed on bacterial inactivation is based on the occurrence of very specific damage on DNA and other essential components such as proteins, lipids, membrane, *etc.*, that inhibits its duplication and consequently bacterial reproduction. The typical UVC damage induces the formation of thymine–thymine cyclobutane cys–syn thymine–thymine photodimers and pyrimidine (6–4) pyrimidine photoproducts



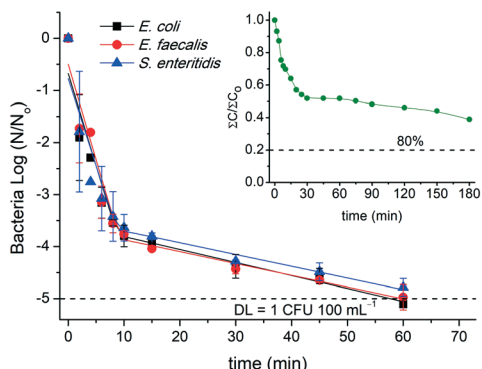


**Fig. 2** Simultaneous bacterial inactivation and MC degradation (inset) under UVC radiation in SMWW secondary effluent as a function of treatment time. Dashed lines refer to detection limit (DL = 1 CFU 100 mL<sup>-1</sup>) and 80% removal of total MCs ( $\sum C_t/\sum C_0$ ).

(TT (6–4) photoproducts).<sup>51</sup> No significant differences in the irradiation time required (60 min) to reach the detection limit (DL) and in the calculated pseudo-first order kinetic constants ( $k$ ) of bacterial inactivation were observed. A double log-linear kinetic characterized by a fast inactivation in the first stage ( $k_1$ ) followed by a slow second inactivation stage ( $k_2$ ) was observed for all bacteria (see Fig. 2). The  $k_1$  for *E. coli*, *E. faecalis*, and *S. enteritidis* were  $3.5 \pm 0.6 \times 10^{-1}$ ,  $3.6 \pm 0.5 \times 10^{-1}$ , and  $3.3 \pm 0.7 \times 10^{-1} \text{ min}^{-1}$ , respectively, while the second stage,  $k_2$ , was around  $0.23 \pm 0.02 \times 10^{-1} \text{ min}^{-1}$  for all pathogens. Clearly, the inactivation process is governed by the first stage. In addition, for all bacteria, the accumulative UVC energy needed to reduce 5 log the initial concentration ( $10^5 \text{ CFU } 100 \text{ mL}^{-1}$ ) was around  $1.2 \text{ kJ L}^{-1}$  and  $0.09 \text{ kJ L}^{-1}$  for a 3.5 log reduction (around 8 min of illumination). Similarly, Rodríguez-Chueca *et al.*<sup>17</sup> did not observe differences in the energy consumption for *E. coli* and *E. faecalis* inactivation under UVC irradiation using real and simulated wastewater. In that paper, a 3.5 log reduction in bacteria concentration demanded  $0.057 \text{ kJ L}^{-1}$  of UVC energy, working in continuous flow mode but at laboratory scale. The upper energy consumption reported in the present work might come from the scaling-up to pilot plant scale as well as differences in the reactor design setup.

Increase of temperature resulting from the operation of the UVC lamp was also monitored during all experiments and the maximum-recorded T remained around 30 °C. This temperature range did not affect the bacterial viability since temperatures higher than 45 °C are necessary to generate thermal damage on the investigated bacteria.<sup>52,53</sup> In addition, this temperature interval should not increase the efficiency of UVC/H<sub>2</sub>O<sub>2</sub> or UVC/S<sub>2</sub>O<sub>8</sub><sup>2-</sup> processes, as temperatures higher than 40 °C and 50 °C, respectively, are normally required.<sup>54,55</sup>

Under certain conditions, UVC light has no effect on the cell wall as the mechanisms of self-repair of microorganisms reverse the DNA damage produced by light absorption.<sup>8</sup> As the UVC process does not generate residual oxidants, reactivation of injured microorganisms is expected if favorable conditions are presented; such as the presence of nutrients related to wastewater (*e.g.*, organic matter and

inorganic salts) that provide a food source for bacteria, allowing them to metabolize and reproduce.<sup>56</sup> Therefore, bacterial regrowth was analyzed in selected samples of experiments (shown in Fig. 2) stored in the dark after 24, 48, and 144 h (6 days) at room temperature. Although an apparent complete inactivation of *E. coli*, *E. faecalis*, and *S. enteritidis* was attained within 60 min under UVC irradiation, regrowth assessment in samples collected after 75 min of UVC treatment was carried out for all bacterial strains. *E. coli* had an exponential increase in the concentration of viable bacteria after 48 and 144 h in the dark, with values of 2.3 and 3.5 log, respectively. In contrast, the regrowth assessment for *S. enteritidis* decreased from 1.1 log in 48 h to 0.2 log after 144 h, probably due to the lack of essential nutrients for its viability. Regrowth assessment for *E. faecalis* was not done in the stored samples after 24 and 48 h, but it was observed (1 log) after 144 h. These regrowth tests offer a good evaluation of the effectiveness of a process and the ability to handle post-treated effluents, which could remain stored in the dark several days before its further reuse. In this sense, UVC technology is not fully recommended for municipal wastewater secondary effluent disinfection, even less for reclaimed final purposes.

On the other hand, the inset in Fig. 2 shows the degradation profile for the sum of MC concentrations ( $\sum C_t/\sum C_0$ ) in the SMWW secondary effluent during the UVC process. For analysis purposes and considering, as an example, environmental regulations already established in Switzerland for MC elimination from MWWTPs, experiments were performed with the aim of removing 80% of total MCs.<sup>57,58</sup> UVC radiation significantly decreased the total amount of MCs (60%) in the effluent after 180 min (3.8 kJ L<sup>-1</sup> accumulative UVC radiation required); however, it was not enough to attain the degradation target of 80%. Clearly, some MCs demanded a longer irradiation time (and so higher accumulative UVC energy) to be oxidized than that required for reaching complete bacterial inactivation, but others were slightly affected by UVC irradiation. However, it is important to highlight that though complete elimination of the sum of MCs was not achieved, some of them attained degradation percentages higher than 75%. This behavior is in agreement with the different absorption capacities of UVC light by the organic compounds, measured by the quantum yield and the molar absorption coefficient at 254 nm. These two fundamental parameters govern the direct photolysis rate; thus, molecules with moderate values of these parameters will be more sensitive to degradation under UVC irradiation. The chemical structures, absorbance (at 254 nm), quantum yields, molar absorption coefficients, and UV absorption spectrum of these compounds can be seen in Table S2 and Fig. S2.† In this sense, DCF and SMX, with high values of these parameters at 254 nm, were substantially removed (<DL) in the beginning of the experiment, *i.e.*, in 20 min (0.3 kJ L<sup>-1</sup> accumulative UVC energy) and 30 min (0.6 kJ L<sup>-1</sup> accumulative UVC energy), respectively. On the other hand, 75% of ACT was removed only after 180 min (3.8 kJ L<sup>-1</sup> of



accumulative UVC energy), while CBZ, CAF, and TMP showed the lowest degradation percentages (20%, 30%, and 40%, respectively) since they have low molar absorption and quantum yield. These results are in accordance with the findings of Yu *et al.*,<sup>9</sup> which classified several pollutants based on their relative reactivity towards UVC direct photolysis. DCF and SMX were considered easily photodegraded by UVC light with no additional oxidants, whereas CAF, CBZ, and TMP were classified as photo-resistant but highly reactive with HO<sup>•</sup> radicals. Cerreta *et al.*<sup>18</sup> also reported that SMX was almost completely removed in natural and distilled water after 30 min of treatment (90%; 0.7 kJ L<sup>-1</sup> accumulative UVC energy) using only UVC, while only 18% of CBZ degradation was observed after 120 min (2.7 kJ L<sup>-1</sup> accumulative UVC energy). Other parameters such as pH, conductivity, turbidity, DOC, DIC, and ion concentration were also monitored but had an insignificant variation throughout the experiments, as expected (data not shown). It is important to mention that specifically, a decrease in the organic load (measured by COD) is expected to provoke an increase of light penetration in the system. Consequently, this might result in an improvement of UVC-based AOP efficiency considering MC removal and bacterial inactivation.

### 3.2 UVC/H<sub>2</sub>O<sub>2</sub> treatment for simultaneous bacterial inactivation and MC elimination

Fast inactivation rates of *E. coli*, *E. faecalis*, and *S. enteritidis* were observed for UVC/H<sub>2</sub>O<sub>2</sub> experiments in all concentrations investigated (5–50 mg L<sup>-1</sup>), as it can be observed in Fig. 3. Similar to the UVC results, double log-linear kinetics was observed for all bacterial inactivation. However, in comparison with these results, the addition of H<sub>2</sub>O<sub>2</sub> did not entail an improvement in the disinfection process since the pseudo-first-order inactivation kinetic constants ( $k_1$  and  $k_2$ ) did not show a significant increase (see Table 2). Only at higher H<sub>2</sub>O<sub>2</sub> concentrations (25, 35, and 50 mg L<sup>-1</sup>), it was observed a slight increase in the inactivation kinetic constants and a reduction in the irradiation time to attain the DL. In particular, for 25 mg L<sup>-1</sup> H<sub>2</sub>O<sub>2</sub>, bacterial inactivation was very fast in the first stage, so it was not possible to fit the curve to calculate  $k_1$ . According to these results, the main inactivation mechanism came from the effect of UVC radiation rather than from damage produced by HO<sup>•</sup> generated through H<sub>2</sub>O<sub>2</sub> photolysis.

Similarly, Pablos *et al.*<sup>19</sup> and Yoon *et al.*<sup>59</sup> suggested that the germicidal effect of UVC absorption by bacterial DNA in *E. coli* K12 and DH5 $\alpha$  strains, respectively, is the main inactivation mechanism and no significant differences were observed in the values of  $k$  for UVC and UVC/H<sub>2</sub>O<sub>2</sub>. Moussavi *et al.*<sup>60</sup> also reported that the enhancement on inactivation of *E. coli* by adding H<sub>2</sub>O<sub>2</sub> was hardly noticeable compared to UVC in the treatment of hospital wastewater. In contrast, Rubio *et al.*<sup>61</sup> reported a significant enhancement in *E. coli* K12 inactivation in natural water after addition of H<sub>2</sub>O<sub>2</sub> compared to the use of only UVC light. The  $k$  increased 150%



Fig. 3 Effect of H<sub>2</sub>O<sub>2</sub> concentration on the *E. coli* (a), *E. faecalis* (b), and *S. enteritidis* (c) inactivation by UVC/H<sub>2</sub>O<sub>2</sub> as a function of treatment time in SMWW secondary effluent. Dashed lines refer to detection limit (DL = 1 CFU per 100 mL<sup>-1</sup>).

for the combined process. Moreover, Moreno-Andrés *et al.*<sup>62</sup> indicated that the addition of H<sub>2</sub>O<sub>2</sub> (10 mg L<sup>-1</sup>) to the UVC system improved the disinfection efficiency of *E. faecalis* in salty water. Probably, the sum of the effects of UVC irradiation and HO<sup>•</sup> species was the major route for bacterial inactivation in those studies, and in other cases HO<sup>•</sup> species compensated for the absorption of photons at 254 nm by H<sub>2</sub>O<sub>2</sub>.

The inactivation efficiency of microorganisms using this process may also depend on many factors, such as the hydrodynamic parameters of the photoreactor, power of the UVC lamp (or UVC energy dose), light path length of the



**Table 2** Pseudo-first-order kinetic constants ( $k$ ) for simultaneous inactivation of bacteria and MC degradation in a SMWW secondary effluent by a UVC/H<sub>2</sub>O<sub>2</sub> process

Process UVC/H <sub>2</sub> O <sub>2</sub> (mg L <sup>-1</sup> )	Bacteria – $k_1/k_2$ (10 <sup>-1</sup> min <sup>-1</sup> )			Total MCs – $k$ (10 <sup>-2</sup> min <sup>-1</sup> )		
	<i>E. coli</i>	<i>E. faecalis</i>	<i>S. enteritidis</i>	( $\sum C_i/\sum C_0$ )	Time <sup>a</sup> (min)	$Q_{UVC}$ <sup>b</sup> (kJ L <sup>-1</sup> )
0	3.5 ± 0.6 (0.86)/0.24 ± 0.02 (0.97)	3.6 ± 0.5 (0.90)/0.23 ± 0.02 (0.96)	3.3 ± 0.7 (0.87)/0.22 ± 0.02 (0.97)	0.5 (0.82) only 60%	180	3.8
5	3.7 ± 0.5 (0.90)/0.27 ± 0.04 (0.90)	4.0 ± 0.5 (0.93)/0.19 ± 0.04 (0.81)	3.5 ± 0.5 (0.90)/0.30 ± 0.02 (0.98)	1.2 (0.94)	120	2.5
15	3.9 ± 0.6 (0.88)/0.19 ± 0.04 (0.77)	3.9 ± 0.5 (0.91)/0.25 ± 0.04 (0.89)	3.8 ± 0.4 (0.94)/0.24 ± 0.04 (0.86)	3.0 (0.97)	52	1.0
25	ND/0.33 ± 0.03 (0.93)	ND/0.45 ± 0.4 (0.95)	ND/0.44 ± 0.04 (0.94)	5.7 (0.99)	24	0.4
35	5.6 ± 0.9 (0.93)/0.18 ± 0.02 (0.91)	4.1 ± 0.7 (0.89)/0.25 ± 0.01 (0.98)	3.8 ± 0.7 (0.87)/0.25 ± 0.02 (0.97)	7.0 (0.99)	21	0.4
50	4.8 ± 0.9 (0.88)/0.26 ± 0.03 (0.96)	4.2 ± 0.5 (0.92)/0.21 ± 0.01 (0.97)	5.3 ± 0.4 (0.97)/0.27 ± 0.03 (0.93)	10.0 (0.99)	17	0.3

<sup>a</sup> Values refer to the attainment of 80% removal of total MCs except for the UVC alone experiment, in which only 60% of total MC removal was attained. <sup>b</sup> Accumulative UVC energy required to attain 80% removal of total MCs. Values in parentheses refer to coefficient of determination ( $R^2$ ). ND = not determined.

photoreactor, water matrix, oxidant concentration, type of bacterial strains, etc. Moreno-Andrés<sup>62</sup> also reported a detrimental effect on bacterial inactivation due to the addition of a high concentration of H<sub>2</sub>O<sub>2</sub> (100 mg L<sup>-1</sup>) based on the competition for the absorption of photons at 254 nm between bacteria and the oxidant. This detrimental effect was not observed under the operating conditions used in this work, which would probably appear at higher concentrations of H<sub>2</sub>O<sub>2</sub> or longer light path length in which the competition for photon absorption would be significantly higher (see section 3.4).

It is important to note that the photolysis percentage of H<sub>2</sub>O<sub>2</sub> was only 10% after 60 min independently of the concentration used. This means a consumption rate of 0.008, 0.045, and 0.076 mg H<sub>2</sub>O<sub>2</sub> L<sup>-1</sup> min<sup>-1</sup> for 5, 25 and 50 mg L<sup>-1</sup>, respectively, which explain the poor contribution of low H<sub>2</sub>O<sub>2</sub> concentrations on bacterial inactivation in comparison with the UVC effect.

In this case, for concentrations between 25 and 50 mg L<sup>-1</sup>, high residual concentrations of this oxidant were present in the treated wastewater. This suggests that the slight enhancement on bacterial inactivation observed at high concentrations might be due to a small fraction of HO<sup>•</sup> generated or to the direct disinfectant effect of H<sub>2</sub>O<sub>2</sub>, since it is well known that at high concentrations this oxidant has a toxic effect on bacterial viability. Rodríguez-Chueca *et al.*<sup>52</sup> reported 6 log and 1.5 log reduction of *E. coli* and *E. faecalis*, respectively, after 180 min in the dark using 50 mg L<sup>-1</sup> of H<sub>2</sub>O<sub>2</sub>. At lower concentrations (20 mg L<sup>-1</sup>) this effect is not significant on inactivation of *E. coli* O157:H7 and *S. enteritidis*, as reported by Nahim-Granados *et al.*<sup>53</sup>

As discussed in the UVC reference experiment, bacterial regrowth was monitored in the treated samples due to their self-repair capacity in the dark. In the presence of H<sub>2</sub>O<sub>2</sub>, regrowth was not observed after the treatment (sample withdrawn after 75 min) under any of the conditions tested (5–50 mg L<sup>-1</sup>) and for all times analyzed (24, 48 and 144 h). H<sub>2</sub>O<sub>2</sub> concentration in all experiments remained constant in

the dark until 144 h of storage. Therefore, the remaining H<sub>2</sub>O<sub>2</sub> has a possible further bacteriostatic effect, preventing bacterial repair/reproduction during the storage or through the distribution system. Other studies report assessment of bacterial regrowth but only after 24 and 48 h.<sup>17,63,64</sup>

The effect of H<sub>2</sub>O<sub>2</sub> concentration on MC degradation was also evaluated (Fig. 4). The use of H<sub>2</sub>O<sub>2</sub> in combination with UVC irradiation increased the removal of all target compounds compared with UVC alone, especially those that are photo-stable, CAF, CBZ, and TMP, resulting in a degradation rate of over 80% for the sum of MCs under all investigated conditions. This effect was mainly caused by the effect of HO<sup>•</sup> generated in H<sub>2</sub>O<sub>2</sub> photolysis at 254 nm (see eqn (1)). Illumination time (and accumulative UVC energy) required to achieve 80% MC degradation decreased with the increase in H<sub>2</sub>O<sub>2</sub> concentration, *e.g.*, from 120 min (2.5 kJ L<sup>-1</sup> accumulative UVC energy required) with 5 mg L<sup>-1</sup> to 17 min (0.3 kJ L<sup>-1</sup> accumulated UVC energy) with 50 mg L<sup>-1</sup> H<sub>2</sub>O<sub>2</sub> (Table 2).

Clearly, UVC/H<sub>2</sub>O<sub>2</sub> at 5 mg L<sup>-1</sup> required a higher UVC energy dose to degrade MCs than that required for reaching complete bacterial inactivation. Pseudo-first-order kinetic

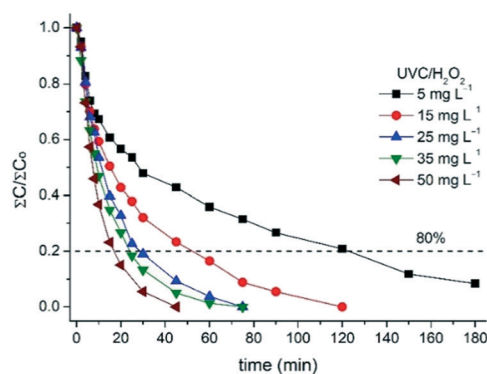


**Fig. 4** Effect of H<sub>2</sub>O<sub>2</sub> concentration on the total MC degradation by UVC/H<sub>2</sub>O<sub>2</sub> as a function of treatment time in SMWW secondary effluent. Dashed line refers to 80% removal of total MCs ( $\sum C_i/\sum C_0$ ).



constants ( $k$ ) corresponding to these experiments are also shown in Table 2. It was noticed that the degradation kinetic constants of this process were strongly dependent on the initial concentration of the oxidant. That behavior can be observed in Fig. S3,† which shows a linear relationship between kinetic constants and initial concentrations of  $\text{H}_2\text{O}_2$ . Despite this, it is important also to highlight that while kinetic constants increased proportionally with  $\text{H}_2\text{O}_2$  till  $0.1 \text{ min}^{-1}$  for  $50 \text{ mg L}^{-1} \text{ H}_2\text{O}_2$ , the illumination time required to reach 80% of degradation varied slightly when using 35 and  $25 \text{ mg L}^{-1} \text{ H}_2\text{O}_2$  and ranged from 21 to 24 min, respectively. In addition, oxidant residual concentrations after treatment were 49 and  $23 \text{ mg L}^{-1}$  for 50 and  $25 \text{ mg L}^{-1} \text{ H}_2\text{O}_2$ , respectively, showing a limitation caused by the light path length and therefore by the photoreactor configuration, which will be addressed in section 3.4.

For a better understanding of the effect of the UVC/ $\text{H}_2\text{O}_2$  process on MC removal, the degradation profile of each compound and the oxidant consumption are detailed in Fig. S4.† Moreover, Table S3† shows the calculated  $k$  for each contaminant as a function of  $\text{H}_2\text{O}_2$  concentration used. CAF, TMP, and CBZ, which did not exhibit a high photodegradation percentage (20–40%), were significantly removed using  $5 \text{ mg L}^{-1} \text{ H}_2\text{O}_2$  under UVC irradiation, attaining removal rates of over 80% after 180 min and with a  $\text{H}_2\text{O}_2$  consumption close to  $1.0 \text{ mg L}^{-1}$ . For this condition, only  $0.8 \text{ mg L}^{-1} \text{ H}_2\text{O}_2$  and  $2.5 \text{ kJ L}^{-1}$  were required to eliminate 80% of the total MCs. A higher increase in the degradation rate was observed for UVC/ $\text{H}_2\text{O}_2$  with  $25 \text{ mg L}^{-1}$ , reaching 80% of removal in 24 min and consuming  $2.3 \text{ mg L}^{-1}$  of the oxidant. As expected, 80% of total MCs was quickly achieved using  $50 \text{ mg L}^{-1}$  (17 min;  $0.3 \text{ kJ L}^{-1}$  accumulated UVC energy) with a  $\text{H}_2\text{O}_2$  consumption of  $1.3 \text{ mg L}^{-1}$ . Similar values were also found by Miralles-Cuevas *et al.*<sup>65</sup> for 90% removal of several MCs. The complete elimination (<DL) of all MCs was attained in 60 min ( $1.2 \text{ kJ L}^{-1}$  accumulated UVC energy) and using  $4.6 \text{ mg L}^{-1} \text{ H}_2\text{O}_2$ . It is important to note that for the same process, the degradation kinetic constant for the photo-stable compounds did not show significant differences, which confirm the non-selectivity of the generated  $\text{HO}^\bullet$  species by the  $\text{H}_2\text{O}_2$  homolysis. On the other hand, DOC decreased around 10% only for high concentrations of  $\text{H}_2\text{O}_2$  ( $25\text{--}50 \text{ mg L}^{-1}$ ; data not shown).

### 3.3 UVC/ $\text{S}_2\text{O}_8^{2-}$ treatment for simultaneous bacterial inactivation and MC degradation

*E. coli*, *E. faecalis*, and *S. enteritidis* inactivation by the UVC/ $\text{S}_2\text{O}_8^{2-}$  process is shown in Fig. 5. As it can be observed, *E. coli* was quickly inactivated under the two investigated conditions, improving significantly the pseudo-first-order kinetic constants obtained with the UVC process (see Table 3). Due to the high rate of *E. coli* inactivation under these conditions, it was not possible to calculate the kinetic constants  $k_1$  (first stage). DL was achieved only after 10 min ( $0.1 \text{ kJ L}^{-1}$  accumulated UVC energy) and 15 min ( $0.2 \text{ kJ L}^{-1}$

accumulated UVC energy) for 40 and  $20 \text{ mg L}^{-1} \text{ S}_2\text{O}_8^{2-}$ , respectively. Several studies attributed the bacterial inactivation in the UVC/ $\text{S}_2\text{O}_8^{2-}$  system to the selectivity and reactivity of generated  $\text{SO}_4^{\cdot-}$  species (see eqn (2)), which reacts with macromolecules that are present in the cell wall. Michael-Kordatou *et al.*<sup>66</sup> reported a significant enhancement (around 200%) to reduced 5-log of *E. coli* in urban wastewater after the addition of  $\text{S}_2\text{O}_8^{2-}$ . Popova *et al.*<sup>67</sup> also reported an increase (>130%) in the rate constant to eliminate *E. coli* when using the UVC/ $\text{S}_2\text{O}_8^{2-}$  process.

On the other hand, comparison with systems based on the generation of  $\text{HO}^\bullet$ , such as UVC/ $\text{H}_2\text{O}_2$ , is difficult to address.

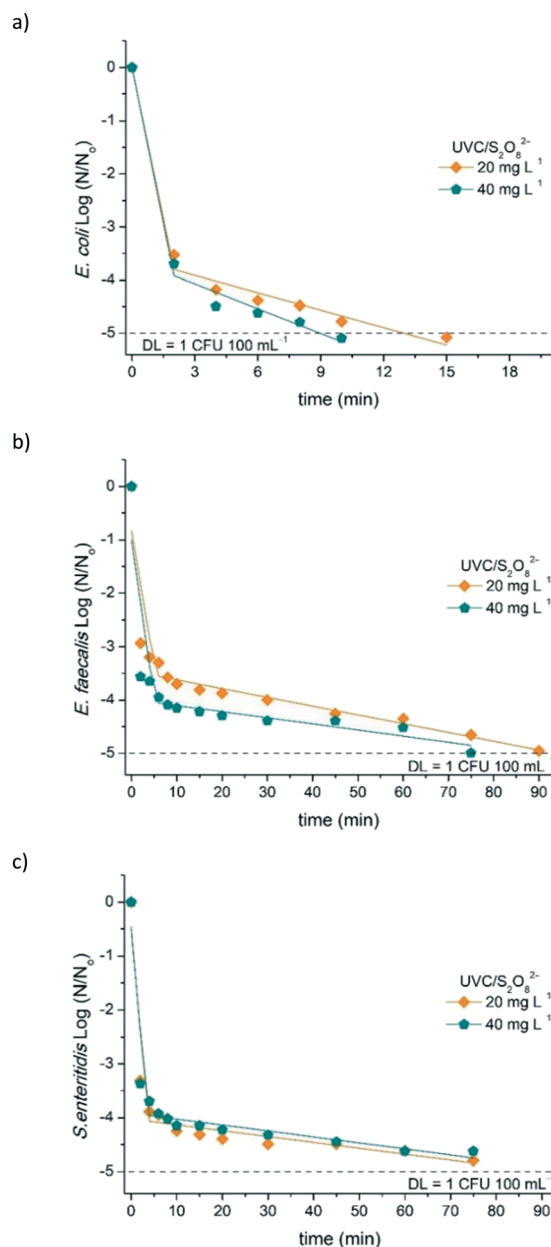


Fig. 5 Effect of  $\text{S}_2\text{O}_8^{2-}$  concentration on the *E. coli* (a), *E. faecalis* (b), and *S. enteritidis* (c) inactivation by UVC/ $\text{S}_2\text{O}_8^{2-}$  as a function of treatment time in SMWW secondary effluent. Dashed lines refer to detection limit (DL = 1 CFU per 100 mL<sup>-1</sup>).





**Table 3** Pseudo-first-order kinetic constants (*k*) for simultaneous inactivation of bacteria and MC degradation in a SMWW secondary effluent by the UVC/S<sub>2</sub>O<sub>8</sub><sup>2-</sup> process

Process (mg L <sup>-1</sup> )	Bacteria – <i>k</i> <sub>1</sub> / <i>k</i> <sub>2</sub> (10 <sup>-1</sup> min <sup>-1</sup> )			Total MCs – <i>k</i> (10 <sup>-2</sup> min <sup>-1</sup> )		
	<i>E. coli</i>	<i>E. faecalis</i>	<i>S. enteritidis</i>	(∑ <i>C</i> <sub>i</sub> /∑ <i>C</i> <sub>0</sub> )	Time <sup>a</sup> (min)	<i>Q</i> <sub>UVC</sub> <sup>b</sup> (kJ L <sup>-1</sup> )
0	3.5 ± 0.6 (0.86)/0.24 ± 0.02 (0.97)	3.6 ± 0.5 (0.90)/0.23 ± 0.02 (0.96)	3.3 ± 0.7 (0.87)/0.22 ± 0.02 (0.97)	0.5 (0.82) only 60%	180	3.8
20	ND/1.1 ± 0.1 (0.87)	5.1 ± 2.1 (0.53)/0.2 ± 0.01 (0.95)	6.2 ± 2.7 (0.59)/0.1 ± 0.02 (0.80)	1.6 (0.99)	90	1.8
40	ND/1.5 ± 0.3 (0.84)	6.0 ± 2.8 (0.52)/0.1 ± 0.01 (0.87)	6.0 ± 2.7 (0.57)/0.1 ± 0.01 (0.92)	4.2 (0.98)	45	0.9
100	NM	NM	NM	11.6 (0.98)	24	0.4

<sup>a</sup> Values refer to the attainment of 80% removal of total MCs except for the UVC alone experiment, in which only 60% of total MC removal was attained. <sup>b</sup> Accumulative UVC energy required to attain 80% removal of total MCs. Values in parentheses refer to coefficient of determination (*R*<sup>2</sup>). ND = not determined. NM = not measured.

From a purely chemical approach, the best option is to compare the efficiency of these systems using an equivalent molar ratio of both oxidants, but the high S<sub>2</sub>O<sub>8</sub><sup>2-</sup> molar mass implies very high concentrations in terms of mass per unit of volume.<sup>64</sup> This would lead to a drastic increase in the operating costs of this process. In this sense, the focus of this study was to assess the behavior of this system under realistic conditions, rather than strictly compare kinetics with UVC/H<sub>2</sub>O<sub>2</sub>. It must be highlighted that H<sub>2</sub>O<sub>2</sub> and S<sub>2</sub>O<sub>8</sub><sup>2-</sup> selected concentrations were in the range of those successfully studied in previous research works.<sup>17,30,64</sup> In addition, other factors such as the stronger selective oxidation capability towards macromolecules/biomolecules of the cell membrane and the half-life of the produced radical can favor a stronger action of SO<sub>4</sub><sup>•-</sup>.

Wordofa *et al.*<sup>68</sup> showed that exposure to SO<sub>4</sub><sup>•-</sup> promoted the loss of cell viability of *E. coli* O157:H7 5 times faster than when HO<sup>•</sup> was used. This unique feature of SO<sub>4</sub><sup>•-</sup> is possibly associated with its highly selective reactivity towards electron-rich moieties on the surface of *E. coli* O157:H7 cell membranes, such as flagella, proteins, and extracellular polymeric substances. Moreover, Serna-Galvis *et al.*<sup>69</sup> also attributed the microorganism inactivation by UVC/S<sub>2</sub>O<sub>8</sub><sup>2-</sup> to the already commented high interaction of SO<sub>4</sub><sup>•-</sup> with organic macromolecules of the cell wall.

As can be seen in Fig. 5b and c, the UVC/S<sub>2</sub>O<sub>8</sub><sup>2-</sup> system was less effective on *E. faecalis* and *S. enteritidis* inactivation. Both bacteria were inactivated within 75–90 min (1.2–1.5 kJ L<sup>-1</sup> accumulated UVC energy, respectively) for the two tested concentrations. Clearly, this result indicates a different inactivation mechanism, probably related to structural differences and cellular composition between these bacteria. In particular, *E. faecalis*, which required 90 and 75 min to attain the DL using 20 and 40 mg L<sup>-1</sup> of S<sub>2</sub>O<sub>8</sub><sup>2-</sup>, respectively, has a structural difference with *E. coli* regarding the cell wall components. *E. faecalis* has a thicker cell wall in which the major component is the peptidoglycan layer. In contrast, *E. coli* has a thin layer of peptidoglycan together with an outer membrane that results in a more complex structure. These differences make Gram-negative bacteria (*e.g.*, *E. coli*) more sensitive than Gram-positive (*e.g.*, *E. faecalis*) with respect to

UV-based treatments.<sup>63,70</sup> Although both *E. coli* and *S. enteritidis* are Gram-negative bacteria, the latter one showed higher resistance to inactivation, which could be due to the presence of different sugars and sugar linkages that form the lipopolysaccharide,<sup>71</sup> the major component of the Gram-negative bacterial outer membrane. Wordofa *et al.*<sup>68</sup> also reported that the efficiency of these processes are dependent on the specific composition of macromolecules for each bacterial group. Another possible mechanism is related to the detrimental effect on bacteria inactivation based on the competition for the absorption of photons at 254 nm between bacteria and oxidant, since S<sub>2</sub>O<sub>8</sub><sup>2-</sup> has a high capacity of light absorption at this wavelength.<sup>26</sup> While some fundamental investigations on the inactivation of different microorganisms by SO<sub>4</sub><sup>•-</sup> have been established, the molecular mechanisms of inactivation, particularly the interaction of SO<sub>4</sub><sup>•-</sup> with biomolecules, are far from complete comprehension.

Bacterial regrowth assessment was carried out after 24, 48, and 144 h after the treatment was finished. Regrowth for all bacteria was detected for 20 and 40 mg L<sup>-1</sup> S<sub>2</sub>O<sub>8</sub><sup>2-</sup>, but much lower compared with that using only the UVC treatment. In particular, *E. faecalis* and *S. enteritidis* had a maximum regrowth of around 0.7 log after 48 h under both conditions, but it was not detected (<DL) after 144 h of storage. In contrast, *E. coli* regrowth was significant, increasing the concentration of viable bacteria after 24 and 48 h in the dark, until 1.3 and 1.9 log, respectively, remaining almost constant after 144 h. This means that the residual concentration of S<sub>2</sub>O<sub>8</sub><sup>2-</sup>, 18 mg L<sup>-1</sup> (for the initial concentration of 20 mg L<sup>-1</sup>) and 28 mg L<sup>-1</sup> (for the initial concentration of 40 mg L<sup>-1</sup>) did not prevent bacterial regrowth since S<sub>2</sub>O<sub>8</sub><sup>2-</sup> has no bactericidal effect by itself. To check this, several experiments (data not shown) were carried out putting in contact bacteria with S<sub>2</sub>O<sub>8</sub><sup>2-</sup> in different concentrations (up to 50 mg L<sup>-1</sup>) and in the dark. No significant effect was observed on the viability of bacteria. This fact is explained due to the size and charge of S<sub>2</sub>O<sub>8</sub><sup>2-</sup>, which can limit the diffusion through the cell membrane, avoiding the inactivation *via* a Fenton-like reaction, as the case of H<sub>2</sub>O<sub>2</sub>.<sup>72</sup> Moreno-Andrés *et al.*<sup>63</sup> observed regrowth (after 48) for *E. coli* and *E. faecalis* bacteria



in distilled water after UVC/S<sub>2</sub>O<sub>8</sub><sup>2-</sup> treatment, even when using a higher oxidant concentration (200 mg L<sup>-1</sup>) than the used in the present study.

The UVC/S<sub>2</sub>O<sub>8</sub><sup>2-</sup> system was also effective in removing 80% of the sum of MCs (Fig. 6), but in slightly longer treatment times than those obtained with UVC/H<sub>2</sub>O<sub>2</sub>. This result could be justified by the use of S<sub>2</sub>O<sub>8</sub><sup>2-</sup> in a molar concentration lower than that of H<sub>2</sub>O<sub>2</sub>. Therefore, it is important to stress that similar treatment time (24 min; 0.4 kJ L<sup>-1</sup> accumulated UVC energy) was required to eliminate 80% of the sum of MCs with 25 mg L<sup>-1</sup> UVC/H<sub>2</sub>O<sub>2</sub> and 100 mg L<sup>-1</sup> UVC/S<sub>2</sub>O<sub>8</sub><sup>2-</sup>, that means 0.73 mmol L<sup>-1</sup> and 0.52 mmol L<sup>-1</sup>, respectively. Starling *et al.*<sup>73</sup> reported an increase in the removal rates for photo-stable compounds CAF and CBZ in 2 L of a real surface water by using UVC/S<sub>2</sub>O<sub>8</sub><sup>2-</sup> (1 mmol L<sup>-1</sup>), resulting in more than 90% degradation with a UVC energy of 5.9 and 11.8 J L<sup>-1</sup>, respectively. In contrast, DOC concentration had a very slight variation throughout the experiments (data not shown), even when using the higher S<sub>2</sub>O<sub>8</sub><sup>2-</sup> concentration (100 mg L<sup>-1</sup>).

Similar to the UVC/H<sub>2</sub>O<sub>2</sub> process, increase in the oxidant concentration also increased MC removal rates (*k*), (Table 3), achieving 80% of total degradation after 90 min (1.8 kJ L<sup>-1</sup> accumulated UVC energy) when using 20 mg L<sup>-1</sup> S<sub>2</sub>O<sub>8</sub><sup>2-</sup> and only 24 min (0.4 kJ L<sup>-1</sup> accumulated UVC energy) for 100 mg L<sup>-1</sup>. This confirms that the generation of SO<sub>4</sub><sup>•-</sup> plays a major role in the degradation of the six MCs; Fig. S5† shows a linear relationship between the degradation kinetic constants with the initial concentration of S<sub>2</sub>O<sub>8</sub><sup>2-</sup>. In addition, Fig. S6† shows the degradation profile of each contaminant and the S<sub>2</sub>O<sub>8</sub><sup>2-</sup> consumption for all conditions studied.

Similar evolution curves for pseudo-first-order kinetic constants for MC removal were obtained compared to H<sub>2</sub>O<sub>2</sub> tests (see Fig. S8, ESI†), confirming that it was not necessary to check more S<sub>2</sub>O<sub>8</sub><sup>2-</sup> concentrations.

As expected, the degradation curves had a similar profile as UVC/H<sub>2</sub>O<sub>2</sub>. No significant increase in the degradation rates of DCF and SFX were observed; however, TMP was slowly oxidized with regard to the rest of the MCs, contrary to what occurred when UVC/H<sub>2</sub>O<sub>2</sub> was applied (see degradation kinetic constants in Table S4†). This behavior is explained by

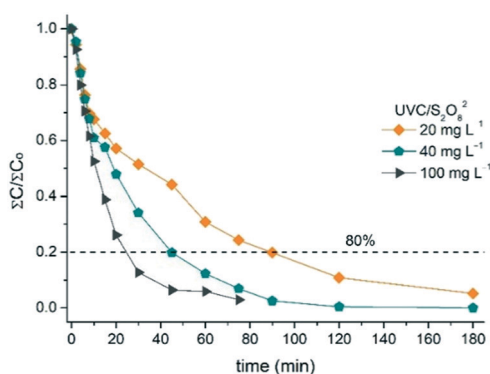


Fig. 6 Effect of S<sub>2</sub>O<sub>8</sub><sup>2-</sup> concentration in the total MC degradation by UVC/S<sub>2</sub>O<sub>8</sub><sup>2-</sup> as a function of treatment time in SMWW secondary effluent. Dashed line refers to 80% removal of total MCs ( $\sum C_t / \sum C_0$ ).

the different reaction rates of SO<sub>4</sub><sup>•-</sup> with specific functional groups of organic molecules. Wojnárovits *et al.*<sup>74</sup> reported that electron-donating substituents increase the rate constants and electron-withdrawing substituents decrease it. In this sense, -OR and -NH<sub>2</sub> (electron-withdrawing substituents) present in the molecular structure of TMP affect the efficiency of SO<sub>4</sub><sup>•-</sup> to degrade this compound. ACT also showed lower kinetic constants due to the effect of these substituents in its structure (-OH and -NHCOR). Once again, this confirms the selective character of generated SO<sub>4</sub><sup>•-</sup> species against the non-selective character of HO<sup>•</sup> generated in UVC/H<sub>2</sub>O<sub>2</sub>. As expected, consumption rates increased with S<sub>2</sub>O<sub>8</sub><sup>2-</sup> initial concentration, attaining 0.04, 0.15, and 0.20 mg S<sub>2</sub>O<sub>8</sub><sup>2-</sup> L<sup>-1</sup> min<sup>-1</sup> for 20, 40 and 100 mg L<sup>-1</sup>, respectively.

### 3.4 Preliminary model to determine the maximum yield of oxidant for UVC-based systems

As reported in this study and in others from the literature, the UVC/H<sub>2</sub>O<sub>2</sub> and UVC/S<sub>2</sub>O<sub>8</sub><sup>2-</sup> processes are very efficient for removing contaminants in aqueous medium. Nevertheless, critical oxidant concentrations seem to be attained and experiments carried out beyond these values are not effective in oxidizing organic compounds. Distinct critical concentrations of H<sub>2</sub>O<sub>2</sub> have been reported as the most suitable since the optimum oxidant concentration is highly dependent on the nature of the target contaminant, water matrix, hydrodynamic parameters of the photoreactor, and power of the UVC lamp.

In Fig. 7a and b, the illumination time required for the removal of 80% of the sum of MCs is shown to be close to 9 min, remaining constant with the increase in the concentration of the oxidant used (H<sub>2</sub>O<sub>2</sub> and S<sub>2</sub>O<sub>8</sub><sup>2-</sup>).

Moreover, the first-order kinetic constant (*k*) showed that adding H<sub>2</sub>O<sub>2</sub> and S<sub>2</sub>O<sub>8</sub><sup>2-</sup> above 150 and 200 mg L<sup>-1</sup>, respectively, did not produce any enhancement in the efficiency of the treatment (see Fig. S7 and S8†). This means that increasing the concentration of the oxidant is not always linked to a treatment improvement due to the self-scavenging reactions (see Table S5†).

On the other hand, the optical path length of the photoreactor plays an important role in the efficiency of these processes, determining the amount of generated radicals. In this sense, the Beer-Lambert law that relates the absorbance with the optical path length and the oxidant concentration can be used to determine the most suitable oxidant quantity for a given photo-reactor setup, as shown in eqn (7):

$$[\text{Ox}] = \frac{A_{254 \text{ nm}}}{\varepsilon_{254 \text{ nm}} \ell} \quad (7)$$

where [Ox] is the oxidant concentration (mg L<sup>-1</sup>),  $\varepsilon$  is the molar absorptivity coefficient of oxidants at 254 nm (mg<sup>-1</sup> L cm<sup>-1</sup>),  $\ell$  is the optical path length of the photo-reactor (cm), and *A* is the absorbance of the solution (including the matrix effect). Here, *A* (0.186 measured at 254 nm) and  $\ell$  (2.595 cm,





Fig. 7 Effect of high concentration of oxidant on the total MC degradation under UVC irradiation as a function of treatment time in SMWW secondary effluent: (a)  $H_2O_2$  and (b)  $S_2O_8^{2-}$ . Dashed lines refer to 80% removal of total MCs ( $\Sigma C_i / \Sigma C_0$ ).

see Fig. 1 for further details, as  $\ell = r_{int,C} - r_{int,L}$  are fixed parameters and depend on the nature of the oxidant.

Taking these parameters into account, the  $H_2O_2$  concentration calculated with eqn (7) is 126 mg L<sup>-1</sup> (3.70 mmol L<sup>-1</sup>) using the molar absorptivity coefficient of  $H_2O_2$  at 254 nm calculated for this system ( $5.7 \times 10^{-4}$  mg<sup>-1</sup> L cm<sup>-1</sup>). This represents a good approximation considering that the experimental concentration for the UVC/ $H_2O_2$  process to attain saturation was 150 mg L<sup>-1</sup>.

As discussed above, the quantum yield of  $S_2O_8^{2-}$  is 2.8 times higher than that of  $H_2O_2$ , so the molar concentration to reach saturation using this oxidant is probably proportional to this factor or lower, *i.e.*, 1.32 mmol L<sup>-1</sup> (or 253 mg of  $S_2O_8^{2-}$  L<sup>-1</sup>). The obtained experimental concentration to attain saturation was 200 mg L<sup>-1</sup> (or 1.04 mmol L<sup>-1</sup>). Additionally, there are many factors to be considered for modelling these systems, such as secondary reactions (including self-scavenging reactions), scavengers present in the matrix, nature of the target contaminants, *etc.* Therefore, the objective of this rough study was only to check the feasibility of a simple equation allowing us to predict the saturation concentration of the oxidants under

the specific experimental conditions used in this investigation.

## Conclusions

The simultaneous elimination of MCs and *E. coli*, *E. faecalis*, and *S. enteritidis* bacteria were attained at pilot plant scale by UVC/ $H_2O_2$  and UVC/ $S_2O_8^{2-}$  processes under operation conditions quite close to actuality. UVC alone was not suitable due to subsequent bacteria regrowth accompanied by a very slow and incomplete removal of MCs.

UVC/ $H_2O_2$  led to a successful bacterial inactivation (without subsequent regrowth) and a simultaneous degradation of MCs up to 99%. By adding 25–50 mg L<sup>-1</sup>  $H_2O_2$ , 4 log of *E. coli*, *E. faecalis*, and *S. enteritidis* bacterial inactivation and MC degradation rate higher than 80% were attained in less than 30 min. In the case of the UVC/ $S_2O_8^{2-}$  process, quicker *E. coli* inactivation was attained due to the possible reaction of generated  $SO_4^{\cdot-}$  with macromolecules in the cell wall. However, regrowth of bacteria was not prevented even when using 50 mg L<sup>-1</sup> in the dark, possibly due to the limitation of  $S_2O_8^{2-}$  diffusion through the cell membrane. When using 20–40 mg L<sup>-1</sup>  $S_2O_8^{2-}$ , 4 log of *E. coli*, *E. faecalis*, and *S. enteritidis* bacterial inactivation was attained in less than 10 min, but achieving more than 80% MC degradation took a longer treatment time than in the UVC/ $H_2O_2$  process. MCs exhibited removal rates proportional to the oxidant concentration used both for UVC/ $H_2O_2$  and for UVC/ $S_2O_8^{2-}$ .

The use of a simple model based on the Beer–Lambert law and taking into account the molar absorptivity of oxidants, as well as water absorbance (matrix effect) and optical length of the photo-reactor, enabled estimation of the maximum concentration of oxidants required to attain maximum oxidation rates in the specific UVC pilot plant used in this study. Further improvements, such as scavenging reactions and water matrix effects, must be considered for a better understanding of the UVC-based processes. Nevertheless, it has been demonstrated that UVC/ $H_2O_2$  and UVC/ $S_2O_8^{2-}$  are able to produce an effluent with enough quality to be reused for several purposes, with agriculture as one of the most suitable end-uses as it is the highest consumer of freshwater worldwide. Nevertheless, it is important to highlight that UVC/ $S_2O_8^{2-}$  process would need a slight addition of bactericidal species to avoid bacterial regrowth along water storage or reclaimed water distribution systems.

## Conflicts of interest

There are no conflicts of interest to declare.

## Acknowledgements

This project has received funding from the European Union's Horizon 2020 research and innovation programme under grant agreement number 820718, and is jointly funded by the European Commission and the Department



of Science and Technology of India (DST). Brazilian funding agencies (Conselho Nacional de Desenvolvimento Científico e Tecnológico – CNPq – grants #142350/2016-8 and #205818/2018-8, Coordenação de Aperfeiçoamento de Pessoal de Nível Superior – CAPES – Finance Code 001, and São Paulo Research Foundation – Fapesp) are also gratefully acknowledged for financial support and scholarships. The authors also wish to thank the Spanish Ministry of Science, Innovation and Universities (MCIU), AEI and FEDER for funding under the CalypSol Project (Reference: RTI2018-097997-B-C32).

## References

- J. M. Galindo-Miranda, C. Guízar-González, E. J. Becerril-Bravo, G. Moeller-Chávez, E. León-Becerril and R. Vallejo-Rodríguez, Occurrence of emerging contaminants in environmental surface waters and their analytical methodology – a review, *Water Supply*, 2019, **19**, 1871–1884.
- M. Biel-Maeso, R. M. Baena-Nogueras, C. Corada-Fernández and P. A. Lara-Martín, Occurrence, distribution and environmental risk of pharmaceutically active compounds (PhACs) in coastal and ocean waters from the Gulf of Cadiz (SW Spain), *Sci. Total Environ.*, 2018, **612**, 649–659.
- Q. Zhang, S. Yang, B. Xie, Z. Jian, C. Deng and R. Hu, Environmental and human health risks assessment of antibiotics residue in drinking water sources: case study of a fast-developing megacity-shenzhen, China, *Water Supply*, 2020, **20**, 499–507.
- C. Caicedo, K. H. Rosenwinkel, M. Exner, W. Verstraete, R. Suchenwirth, P. Hartemann and R. Nogueira, Legionella occurrence in municipal and industrial wastewater treatment plants and risks of reclaimed wastewater reuse: Review, *Water Res.*, 2019, **149**, 21–34.
- P. Roccaro, Treatment processes for municipal wastewater reclamation: The challenges of emerging contaminants and direct potable reuse, *Curr. Opin. Environ. Sci. Health*, 2018, **2**, 46–54.
- M. Salgot and M. Folch, Wastewater treatment and water reuse, *Curr. Opin. Environ. Sci. Health*, 2018, **2**, 64–74.
- O. M. Lee, H. Y. Kim, W. Park, T.-H. Kim and S. Yu, A comparative study of disinfection efficiency and regrowth control of microorganism in secondary wastewater effluent using UV, ozone, and ionizing irradiation process, *J. Hazard. Mater.*, 2015, **295**, 201–208.
- M.-T. Guo and C. Kong, Antibiotic resistant bacteria survived from UV disinfection: Safety concerns on genes dissemination, *Chemosphere*, 2019, **224**, 827–832.
- H.-W. Yu, M. Park, S. Wu, I. J. Lopez, W. Ji, J. Scheideler and S. A. Snyder, Strategies for selecting indicator compounds to assess attenuation of emerging contaminants during UV advanced oxidation processes, *Water Res.*, 2019, **166**, 115030.
- K.-Y. Park, S.-Y. Choi, S.-H. Lee, J.-H. Kweon and J.-H. Song, Comparison of formation of disinfection by-products by chlorination and ozonation of wastewater effluents and their toxicity to *Daphnia magna*, *Environ. Pollut.*, 2016, **215**, 314–321.
- C. Li, D. Wang, X. Xu and Z. Wang, Formation of known and unknown disinfection by-products from natural organic matter fractions during chlorination, chloramination, and ozonation, *Sci. Total Environ.*, 2017, **587–588**, 177–184.
- X.-l. Zhang, H.-w. Yang, X.-m. Wang, J. Fu and Y. F. Xie, Formation of disinfection by-products: Effect of temperature and kinetic modeling, *Chemosphere*, 2013, **90**, 634–639.
- L. Jatzwauk, H. Schöne and H. Pietsch, How to improve instrument disinfection by ultrasound, *J. Hosp. Infect.*, 2001, **48**, S80–S83.
- P. R. Gogate, P. D. Thanekar and A. P. Oke, Strategies to improve biological oxidation of real wastewater using cavitation based pre-treatment approaches, *Ultrason. Sonochem.*, 2020, **64**, 105016.
- T. Leiknes, The effect of coupling coagulation and flocculation with membrane filtration in water treatment: A review, *J. Environ. Sci.*, 2009, **21**, 8–12.
- J. Radjenovic and D. L. Sedlak, Challenges and Opportunities for Electrochemical Processes as Next-Generation Technologies for the Treatment of Contaminated Water, *Environ. Sci. Technol.*, 2015, **49**, 11292–11302.
- J. Rodríguez-Chueca, C. García-Cañibano, R. J. Lepistö, Á. Encinas, J. Pellinen and J. Marugán, Intensification of UV-C tertiary treatment: Disinfection and removal of micropollutants by sulfate radical based Advanced Oxidation Processes, *J. Hazard. Mater.*, 2019, **372**, 94–102.
- G. Cerreta, M. A. Roccamante, I. Oller, S. Malato and L. Rizzo, Contaminants of emerging concern removal from real wastewater by UV/free chlorine process: A comparison with solar/free chlorine and UV/H<sub>2</sub>O<sub>2</sub> at pilot scale, *Chemosphere*, 2019, **236**, 124354.
- C. Pablos, J. Marugán, R. van Grieken and E. Serrano, Emerging micropollutant oxidation during disinfection processes using UV-C, UV-C/H<sub>2</sub>O<sub>2</sub>, UV-A/TiO<sub>2</sub> and UV-A/TiO<sub>2</sub>/H<sub>2</sub>O<sub>2</sub>, *Water Res.*, 2013, **47**, 1237–1245.
- I. J. S. Montes, B. F. Silva and J. M. Aquino, On the performance of a hybrid process to mineralize the herbicide tebuthiuron using a DSA® anode and UVC light: A mechanistic study, *Appl. Catal., B*, 2017, **200**, 237–245.
- R. Xiao, K. Liu, L. Bai, D. Minakata, Y. Seo, R. Kaya Göktaş, D. D. Dionysiou, C.-J. Tang, Z. Wei and R. Spinney, Inactivation of pathogenic microorganisms by sulfate radical: Present and future, *Chem. Eng. J.*, 2019, **371**, 222–232.
- M. Sánchez-Polo, M. M. Abdeldaiem, R. Ocampo-Pérez, J. Rivera-Utrilla and A. J. Mota, Comparative study of the photodegradation of bisphenol A by HO, SO<sub>4</sub><sup>-</sup> and CO<sub>3</sub><sup>-</sup>/HCO<sub>3</sub> radicals in aqueous phase, *Sci. Total Environ.*, 2013, **463–464**, 423–431.
- D. R. Hokanson, K. Li and R. R. Trussell, A photolysis coefficient for characterizing the response of aqueous constituents to photolysis, *Front. Environ. Sci. Eng.*, 2016, **10**, 428–437.
- R. Guan, X. Yuan, Z. Wu, L. Jiang, Y. Li and G. Zeng, Principle and application of hydrogen peroxide based advanced oxidation processes in activated sludge treatment: A review, *Chem. Eng. J.*, 2018, **339**, 519–530.



- 25 D. B. Miklos, R. Hartl, P. Michel, K. G. Linden, J. E. Drewes and U. Hübner, UV/H<sub>2</sub>O<sub>2</sub> process stability and pilot-scale validation for trace organic chemical removal from wastewater treatment plant effluents, *Water Res.*, 2018, **136**, 169–179.
- 26 W. Li, T. Jain, K. Ishida and H. Liu, A mechanistic understanding of the degradation of trace organic contaminants by UV/hydrogen peroxide, UV/persulfate and UV/free chlorine for water reuse, *Environ. Sci.: Water Res. Technol.*, 2017, **3**, 128–138.
- 27 J. L. Weeks and M. S. Matheson, The Primary Quantum Yield of Hydrogen Peroxide Decomposition<sup>1</sup>, *J. Am. Chem. Soc.*, 1956, **78**, 1273–1278.
- 28 F. P. Tully, A. R. Ravishankara, R. L. Thompson, J. M. Nicovich, R. C. Shah, N. M. Kreutter and P. H. Wine, Kinetics of the reactions of hydroxyl radical with benzene and toluene, *J. Phys. Chem.*, 1981, **85**, 2262–2269.
- 29 S. Waclawek, H. V. Lutze, K. Grübel, V. V. T. Padil, M. Černík and D. D. Dionysiou, Chemistry of persulfates in water and wastewater treatment: A review, *Chem. Eng. J.*, 2017, **330**, 44–62.
- 30 S. Guerra-Rodríguez, E. Rodríguez, N. D. Singh and J. Rodríguez-Chueca, Assessment of Sulfate Radical-Based Advanced Oxidation Processes for Water and Wastewater Treatment: A Review, *Water*, 2018, **10**, 1828.
- 31 E. Pelizzetti, V. Carlin, C. Minero and M. Graetzel, Enhancement of the Rate of Photocatalytic Degradation on TiO<sub>2</sub> of 2-Chlorophenol, 2,7-Dichlorodibenzodioxin, and Atrazine by Inorganic Oxidizing Species, *New J. Chem.*, 1991, **15**, 351–359.
- 32 Q. Yang, H. Choi, Y. Chen and D. D. Dionysiou, Heterogeneous activation of peroxymonosulfate by supported cobalt catalysts for the degradation of 2,4-dichlorophenol in water: The effect of support, cobalt precursor, and UV radiation, *Appl. Catal., B*, 2008, **77**, 300–307.
- 33 S. Luo, Z. Wei, D. D. Dionysiou, R. Spinney, W.-P. Hu, L. Chai, Z. Yang, T. Ye and R. Xiao, Mechanistic insight into reactivity of sulfate radical with aromatic contaminants through single-electron transfer pathway, *Chem. Eng. J.*, 2017, **327**, 1056–1065.
- 34 R. Xiao, Z. Luo, Z. Wei, S. Luo, R. Spinney, W. Yang and D. D. Dionysiou, Activation of peroxymonosulfate/persulfate by nanomaterials for sulfate radical-based advanced oxidation technologies, *Curr. Opin. Chem. Eng.*, 2018, **19**, 51–58.
- 35 J. Sharma, I. M. Mishra and V. Kumar, Degradation and mineralization of Bisphenol A (BPA) in aqueous solution using advanced oxidation processes: UV/H<sub>2</sub>O<sub>2</sub> and UV/S<sub>2</sub>O<sub>8</sub><sup>2-</sup> oxidation systems, *J. Environ. Manage.*, 2015, **156**, 266–275.
- 36 E. Kudlek, M. Dudziak and J. Bohdziewicz, Influence of Inorganic Ions and Organic Substances on the Degradation of Pharmaceutical Compound in Water Matrix, *Water*, 2016, **8**, 532.
- 37 J. A. Malvestiti and R. F. Dantas, Influence of industrial contamination in municipal secondary effluent disinfection by UV/H<sub>2</sub>O<sub>2</sub>, *Environ. Sci. Pollut. Res.*, 2019, **26**, 13286–13298.
- 38 USEPA, *Guidelines for Water Reuse*, United States Environmental Protection Agency, Washington, DC, USA, 2012, EPA/600/R-12/618.
- 39 ISO, *Guidelines for Treated Wastewater Use for Irrigation Projects*, International Organization for Standardization, Geneva, Switzerland, 2015, vol. 16075.
- 40 B. Petrie, R. Barden and B. Kasprzyk-Hordern, A review on emerging contaminants in wastewaters and the environment: Current knowledge, understudied areas and recommendations for future monitoring, *Water Res.*, 2015, **72**, 3–27.
- 41 R. Zhang, S. Vigneswaran, H. Ngo and H. Nguyen, A submerged membrane hybrid system coupled with magnetic ion exchange (MIEX®) and flocculation in wastewater treatment, *Desalination*, 2007, **216**, 325–333.
- 42 *Standard Methods for the Examination of Water and Wastewater*, ed. A. D. Eaton and A. E. Greenberg, United Book Press Inc., American Public Health Association; American Waterworks Association, Water Environment Federation, Maryland, USA, 20th edn, 1998.
- 43 C. Liang, C.-F. Huang, N. Mohanty and R. M. Kurakalva, A rapid spectrophotometric determination of persulfate anion in ISCO, *Chemosphere*, 2008, **73**, 1540–1543.
- 44 Royal Decree 1620/2007 (BOE No. 294, 2007), *Concerns of the Legal Regime for the Reuse of Treated Water*, 2007, Available at: <http://www.boe.es/boe/dias/2007/12/08/pdfs/A50639-50661.pdf>.
- 45 J. Marugán, R. van Grieken, C. Sordo and C. Cruz, Kinetics of the photocatalytic disinfection of Escherichia coli suspensions, *Appl. Catal., B*, 2008, **82**, 27–36.
- 46 G. Cerreta, M. A. Roccamante, P. Plaza-Bolaños, I. Oller, A. Agüera, S. Malato and L. Rizzo, Advanced treatment of urban wastewater by UV-C/free chlorine process: Micropollutants removal and effect of UV-C radiation on trihalomethanes formation, *Water Res.*, 2020, **169**, 115220.
- 47 S. Nahim-Granados, G. Rivas-Ibáñez, J. A. Sánchez Pérez, I. Oller, S. Malato and M. I. Polo-López, Synthetic fresh-cut wastewater disinfection and decontamination by ozonation at pilot scale, *Water Res.*, 2020, **170**, 115304.
- 48 E. P. Costa, M. Roccamante, C. C. Amorim, I. Oller, J. A. Sánchez Pérez and S. Malato, New trend on open solar photoreactors to treat micropollutants by photo-Fenton at circumneutral pH: Increasing optical pathway, *Chem. Eng. J.*, 2020, **385**, 123982.
- 49 A. B. Martínez-Piernas, M. I. Polo-López, P. Fernández-Ibáñez and A. Agüera, Validation and application of a multiresidue method based on liquid chromatography-tandem mass spectrometry for evaluating the plant uptake of 74 microcontaminants in crops irrigated with treated municipal wastewater, *J. Chromatogr. A*, 2018, **1534**, 10–21.
- 50 N. H. Tran, M. Reinhard and K. Y.-H. Gin, Occurrence and fate of emerging contaminants in municipal wastewater treatment plants from different geographical regions—a review, *Water Res.*, 2018, **133**, 182–207.
- 51 G. D. Harris, V. D. Adams, D. L. Sorensen and M. S. Curtis, Ultraviolet inactivation of selected bacteria and viruses with photoreactivation of the bacteria, *Water Res.*, 1987, **21**, 687–692.



- 52 J. Rodríguez-Chueca, M. I. Polo-López, R. Mosteo, M. P. Ormad and P. Fernández-Ibáñez, Disinfection of real and simulated urban wastewater effluents using a mild solar photo-Fenton, *Appl. Catal., B*, 2014, **150–151**, 619–629.
- 53 S. Nahim-Granados, J. A. Sánchez Pérez and M. I. Polo-Lopez, Effective solar processes in fresh-cut wastewater disinfection: Inactivation of pathogenic *E. coli* O157:H7 and *Salmonella enteritidis*, *Catal. Today*, 2018, **313**, 79–85.
- 54 S. Yang, P. Wang, X. Yang, L. Shan, W. Zhang, X. Shao and R. Niu, Degradation efficiencies of azo dye Acid Orange 7 by the interaction of heat, UV and anions with common oxidants: Persulfate, peroxymonosulfate and hydrogen peroxide, *J. Hazard. Mater.*, 2010, **179**, 552–558.
- 55 R. L. Johnson, P. G. Tratnyek and R. O. B. Johnson, Persulfate Persistence under Thermal Activation Conditions, *Environ. Sci. Technol.*, 2008, **42**, 9350–9356.
- 56 S. Giannakis, E. Darakas, A. Escalas-Cañellas and C. Pulgarin, Elucidating bacterial regrowth: Effect of disinfection conditions in dark storage of solar treated secondary effluent, *J. Photochem. Photobiol., A*, 2014, **290**, 43–53.
- 57 Federal Office of Environment, *Gewässerqualität: Revision der Gewässerschutzverordnung*, Switzerland, 2017, Available at: <https://www.bafu.admin.ch/bafu/fr/home/themes/formation/communiqués.msg-id-59323.html>.
- 58 M. Bourgin, B. Beck, M. Boehler, E. Borowska, J. Fleiner, E. Salhi, R. Teichler, U. von Gunten, H. Siegrist and C. S. Mc Ardell, Evaluation of a full-scale wastewater treatment plant upgraded with ozonation and biological post-treatments: Abatement of micropollutants, formation of transformation products and oxidation by-products, *Water Res.*, 2018, **129**, 486–498.
- 59 Y. Yoon, H. J. Chung, D. Y. Wen Di, M. C. Dodd, H.-G. Hur and Y. Lee, Inactivation efficiency of plasmid-encoded antibiotic resistance genes during water treatment with chlorine, UV, and UV/H<sub>2</sub>O<sub>2</sub>, *Water Res.*, 2017, **123**, 783–793.
- 60 G. Moussavi, E. Fathi and M. Moradi, Advanced disinfecting and post-treating the biologically treated hospital wastewater in the UVC/H<sub>2</sub>O<sub>2</sub> and VUV/H<sub>2</sub>O<sub>2</sub> processes: Performance comparison and detoxification efficiency, *Process Saf. Environ. Prot.*, 2019, **126**, 259–268.
- 61 D. Rubio, E. Nebot, J. F. Casanueva and C. Pulgarin, Comparative effect of simulated solar light, UV, UV/H<sub>2</sub>O<sub>2</sub> and photo-Fenton treatment (UV-Vis/H<sub>2</sub>O<sub>2</sub>/Fe<sup>2+</sup>,<sup>3+</sup>) in the *Escherichia coli* inactivation in artificial seawater, *Water Res.*, 2013, **47**, 6367–6379.
- 62 J. Moreno-Andrés, L. Romero-Martínez, A. Acevedo-Merino and E. Nebot, Determining disinfection efficiency on *E. faecalis* in saltwater by photolysis of H<sub>2</sub>O<sub>2</sub>: Implications for ballast water treatment, *Chem. Eng. J.*, 2016, **283**, 1339–1348.
- 63 J. Moreno-Andrés, R. Rios Quintero, A. Acevedo-Merino and E. Nebot, Disinfection performance using a UV/persulfate system: effects derived from different aqueous matrices, *Photochem. Photobiol. Sci.*, 2019, **18**, 878–883.
- 64 F. Zeng, S. Cao, W. Jin, X. Zhou, W. Ding, R. Tu, S.-F. Han, C. Wang, Q. Jiang, H. Huang and F. Ding, Inactivation of chlorine-resistant bacterial spores in drinking water using UV irradiation, UV/Hydrogen peroxide and UV/Peroxymonosulfate: Efficiency and mechanism, *J. Cleaner Prod.*, 2020, **243**, 118666.
- 65 S. Miralles-Cuevas, D. Darowna, A. Wanag, S. Mozia, S. Malato and I. Oller, Comparison of UV/H<sub>2</sub>O<sub>2</sub>, UV/S<sub>2</sub>O<sub>8</sub><sup>2-</sup>, solar/Fe(II)/H<sub>2</sub>O<sub>2</sub> and solar/Fe(II)/S<sub>2</sub>O<sub>8</sub><sup>2-</sup> at pilot plant scale for the elimination of micro-contaminants in natural water: An economic assessment, *Chem. Eng. J.*, 2017, **310**, 514–524.
- 66 I. Michael-Kordatou, M. Iacovou, Z. Frontistis, E. Hapeshi, D. D. Dionysiou and D. Fatta-Kassinos, Erythromycin oxidation and ERY-resistant *Escherichia coli* inactivation in urban wastewater by sulfate radical-based oxidation process under UV-C irradiation, *Water Res.*, 2015, **85**, 346–358.
- 67 S. Popova, G. Matafonova and V. Batoev, Simultaneous atrazine degradation and *E. coli* inactivation by UV/S<sub>2</sub>O<sub>8</sub><sup>2-</sup>/Fe<sup>2+</sup> process under KrCl excilamp (222 nm) irradiation, *Ecotoxicol. Environ. Saf.*, 2019, **169**, 169–177.
- 68 D. Wordofa, S. Walker and H. Liu, Sulfate Radical-Induced Disinfection of Pathogenic *Escherichia coli* O157:H7 via Iron-Activated Persulfate, *Environ. Sci. Technol. Lett.*, 2017, **4**, 154–160.
- 69 E. A. Serna-Galvis, L. Salazar-Ospina, J. N. Jiménez, N. J. Pino and R. A. Torres-Palma, Elimination of carbapenem resistant *Klebsiella pneumoniae* in water by UV-C, UV-C/persulfate and UV-C/H<sub>2</sub>O<sub>2</sub>. Evaluation of response to antibiotic, residual effect of the processes and removal of resistance gene, *J. Environ. Chem. Eng.*, 2020, **8**, 102196.
- 70 R. van Grieken, J. Marugán, C. Pablos, L. Furones and A. López, Comparison between the photocatalytic inactivation of Gram-positive *E. faecalis* and Gram-negative *E. coli* faecal contamination indicator microorganisms, *Appl. Catal., B*, 2010, **100**, 212–220.
- 71 W. Wang, A. V. Perepelov, L. Feng, S. D. Shevelev, Q. Wang, S. Senchenkova, W. Han, Y. Li, A. S. Shashkov, Y. A. Knirel, P. R. Reeves and L. Wang, A group of *Escherichia coli* and *Salmonella enterica* O antigens sharing a common backbone structure, *Microbiology*, 2007, **153**, 2159–2167.
- 72 S. Giannakis, M. I. Polo López, D. Spuhler, J. A. Sánchez Pérez, P. Fernández Ibáñez and C. Pulgarin, Solar disinfection is an augmentable, in situ-generated photo-Fenton reaction—Part 1: A review of the mechanisms and the fundamental aspects of the process, *Appl. Catal., B*, 2016, **199**, 199–223.
- 73 M. C. V. M. Starling, P. P. Souza, A. Le Person, C. C. Amorim and J. Criquet, Intensification of UV-C treatment to remove emerging contaminants by UV-C/H<sub>2</sub>O<sub>2</sub> and UV-C/S<sub>2</sub>O<sub>8</sub><sup>2-</sup>: Susceptibility to photolysis and investigation of acute toxicity, *Chem. Eng. J.*, 2019, **376**, 120856.
- 74 L. Wojnárovits and E. Takács, Rate constants of sulfate radical anion reactions with organic molecules: A review, *Chemosphere*, 2019, **220**, 1014–1032.

